Valence and core electronic excitations in LiC_6

L. A. Grunes, I. P. Gates, and J. J. Ritsko*
Xerox Webster Research Center, Building 114, Webster, New York 14580

E. J. Mele and D. P. DiVincenzo
Department of Physics, University of Pennsylvania, Philadelphia, Pennsylvania 19104

M. E. Preil
Laboratory for Research on the Structure of Matter and Department of Physics, University of Pennsylvania, Philadelphia, Pennsylvania 19104

J. E. Fischer
Laboratory for Research on the Structure of Matter and Department of Materials Science and Engineering, University of Pennsylvania, Philadelphia, Pennsylvania 19104

(Received 3 August 1983)

Electron-energy-loss spectroscopy has been used to measure the electronic excitations in LiC_6 from 0.3 to 288 eV. Plasmon losses at 2.85 and 6.3 eV are in good agreement with optical results. In the region between 15 and 40 eV essentially no fine structure associated with backfolded interband transitions is observed contrary to similar measurements in KC_8. These differences are explained by the different bandfolding in MC_6 and MC_8 compounds. The carbon 1*s* absorption edge shows a sharp Fermi-edge discontinuity followed by a shoulder 0.5 eV to higher energy. This 1*s* absorption feature is similar to but weaker than what is seen in MC_8 compounds; while the line shape may be a reflection of C π final-state relaxation, a quantitative understanding of this phenomenon is still lacking. The Li 1*s* absorption edge shows two weak peaks at 57.1 and 58.7 eV, which are assigned to transitions to E_F and to a three-dimensional conduction band, followed by two stronger peaks at 63.0 and 65.2 eV. The latter two exhibit relative intensity changes as a function of orientation leading to their identification as atomiclike transitions to crystal-field-split Li 2*p* levels.

In graphite intercalation compounds the nature and position of alkali-metal—intercalant and graphite π and σ bands has been the subject of recent interest.[1] Positron-annihilation[1] and low-energy photoelectron spectroscopy[2] measurements clearly indicate different valence-band electronic structures for LiC_6 and the heavier-alkali-metal—intercalated graphite compounds MC_8. While the occupation of the three-dimensional metal-derived band of the MC_8 compounds remains controversial,[3] existing experimental evidence[1,2,4] supports the belief that this band is unoccupied in LiC_6. Existing electronic structure calculations also place this band above E_F,[5-7] although they disagree on its atomic origin. We have used electron-energy-loss spectroscopy as a probe of the unoccupied states in LiC_6, as we have done previously for other alkali-graphite compounds.[3,8,9] We observe this three-dimensional conduction band about 1.6 eV above E_F, in good agreement with theory and in qualitative (although not quantitative) agreeement with a recent inverse photoemission study.[10] We have also obtained information about other important unoccupied states in LiC_6. In particular, we obtain additional evidence[8] that the C 3*p* states form a distinguishable band which is backfolded coherently by alkali superlattice effects. Also we identify Li 2*p*—derived states, showing that they remain quite sharp, although they are influenced by crystal-field effects. In general, our results reveal the essentially atomic character of high-lying unoccupied states in these compounds.

The samples were prepared from thin graphite flakes cleaved from large pieces of highly ordered pyrolitic graphite kindly provided by A. Moore of Union Carbide Corporation. The flakes (< 1000 Å thick) were suspended on stainless-steel electron-microscope grids and wrapped in stainless-steel No. 300 screen. Samples were exposed to Li vapor in a sealed stainless-steel tube, some at 400 °C (for minimal carbide formation) and some at 430 °C (for minimal stage-2 contamination) until LiC_6 could be identified by its yellow color in reflection and green color in transmission. The samples were transferred to the electron-energy-loss spectrometer in a pure argon atmosphere. They showed significant deintercalation to stage 2 in the spectrometer vacuum of 2×10^{-8} Torr within 24 h. The data presented here were taken before significant decay was observed.

Electron-energy-loss spectra were recorded from 0.3 to 288 eV with an energy-loss resolution of 0.1 eV. Typical energy-loss spectra of the valence excitations at a momentum transfer of 0.1 Å^{-1} are shown in Fig. 1. The first energy-loss peak at 2.85 eV is the intraband plasmon. The energy of this peak corresponds very well with the sharp dip in reflectivity observed in LiC_6. A Kramers-Kronig analysis produces the ϵ_1 and ϵ_2 of Fig. 2; the inferred

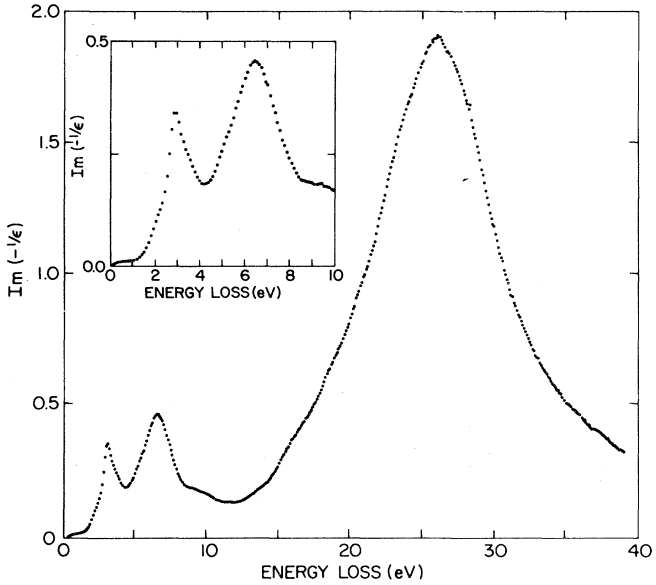

FIG. 1. LiC_6 energy-loss function at $q = 0.1$ Å^{-1} from 0—40 eV.

normal-incidence reflectivity shows reasonable agreement with the direct optical measurements.[11,12] The lack of significant structure below 2.85 eV shows that higher-stage compounds were not present in appreciable amounts. (The very weak shoulder at 2 eV is due to the presence of a stage-2 compound.[12] Growth of this feature with time was used to diagnose deintercalation.) The next peak in the spectrum is the interband plasmon at 6.3 eV. This feature, which is common to all graphite intercalation compounds,[8,9] is basically the response to the π interband excitations which the Kramers-Kronig calculation shows have a peak in ϵ_2 at 4.35 eV; this peak position is similar to KC_8.[9] Between the interband plasmon and the all-valence-electron plasmon at 25.9 eV there are weak peaks at 9.7 and 13 eV. The 13-eV structure is common to all stage-1 alkali-metal—graphite compounds[8,9] and is associated with the graphite σ interband excitations. The corresponding $\sigma \rightarrow \sigma^*$ peak in ϵ_2 occurs at 13.3 eV.[13] In MC_8 compounds this peak is about 1 eV lower, showing that non-rigid-band effects are present even for the σ bands.[4] The weak peak at 9.7 eV corresponds to structure observed at ~ 8 eV in optical reflectivity[11] which arises from several closely spaced interband transitions predicted by theory (Ref. 6, especially Table V).

As Fig. 1 shows, the energy-loss function for LiC_6 lacks any significant fine structure between 15 and 40 eV. By comparison, the MC_8 compounds show many peaks and shoulders associated with metal core-level excitations and excitations of backfolded graphite bands.[8,9] The present observation supports the previous assignment of this MC_8 structure to interband transitions from the bottom of the $2p$ (π) band at Γ to excited states in the $3p$ (π) manifold. These $3p$ states have high density of states at point Q (or M) in the Brillouin zone of graphite; in the MC_8 compounds these Q-point states are folded back to Γ, resulting in a set of strongly allowed interband transitions with high joint densities of states. In LiC_6 the related states map back to point Q in the folded zone.[6] Therefore, these interband transitions are forbidden and a structureless spectrum is predicted (and observed) in this energy region.

Figure 3 shows the C 1s absorption edge in LiC_6 as compared with that in MC_8 compounds.[9,13] Apart from a weak peak at 284.2 eV, which is probably due to a small amount of Li carbide or other impurity,[14] the overall shape of the absorption edge in LiC_6 is similar to that in the MC_8 compounds, and the threshold energies are identical to within 0.2 eV. The peak at the Fermi energy for all these spectra is much broader than in pristine graphite. A simple model for this absorption may be constructed by

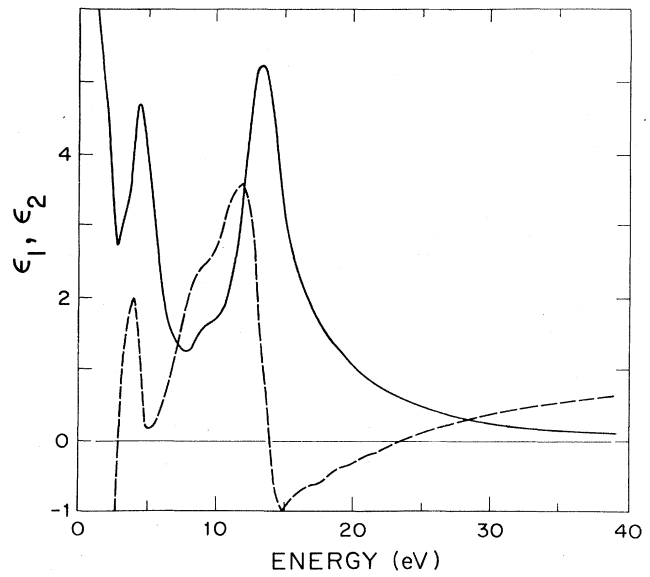

FIG. 2. $\epsilon_1(\omega)$ (dashed) and $\epsilon_2(\omega)$ (solid) for LiC_6 from 0—40 eV as inferred from Kramers-Kronig analysis of Fig. 1.

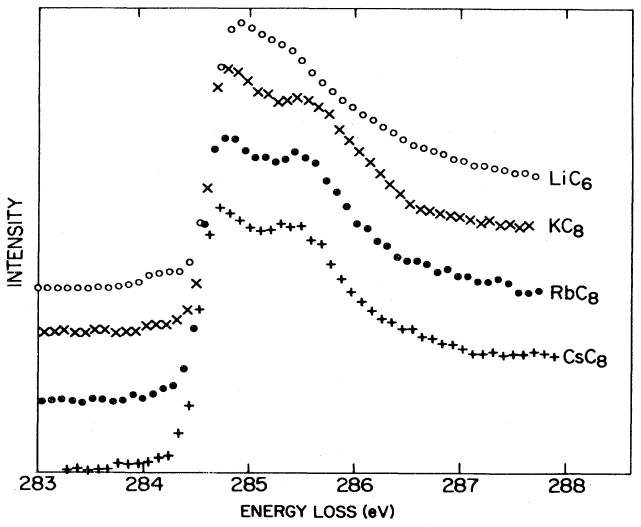

FIG. 3. C 1s core-excitation spectra for LiC_6 compared to KC_8, RbC_8, and CsC_8.

modifying an existing calculation of the x-ray absorption edge in pure graphite using the final-state rule.[15] We may estimate the absorption-edge shape in the donors by simply raising E_F from its pure graphite value. However, this predicts a Fermi-energy peak which is *narrower* than pure graphite, in disagreement with the present experiment. This disagreement results largely from the differences in the final-state screening in the metallic donor compounds as compared with the semimetallic graphite.[16]

In addition to the threshold peak each of the spectra in Fig. 3 shows a second distinguishable structure at high energy. The MC_8 compounds show a peak 0.7 eV above the maximum of the absorption edge. In LiC_6 this shoulder is weaker and appears as a break in slope at 0.5 eV above the absorption edge. This feature is not likely to be the three-dimensional conduction band which appears near the Fermi level in the intercalation compounds[5–7] since these states have negligible overlap with the carbon 1*s* core states. The shoulder might be associated with splitting of the *M*-point density of states which can be substantial[17] due to the *A-A*—layer stacking. However, this effect would be strongest in LiC_6 where the interlayer spacing is smaller than in the MC_8 compounds in contradiction with the experimental results. It is also possible that the shoulder above the absorption edge results from hybridization of metal and carbon wave functions near the Fermi level,[13] with differences in band folding and in metallic wave functions accounting for the weaker shoulder in LiC_6 than in the MC_8 compounds. Still, the close similarity between the three MC_8 spectra argues that the line shape is determined more by an intrinsic C-plane effect rather than by an intercalant-specific response. For example, the shape of the absorption could be determined by the relaxation of the C π conduction electrons to the core hole. While all of these effects are likely to influence the C 1*s* spectra, a detailed understanding of all of its features does not yet exist.

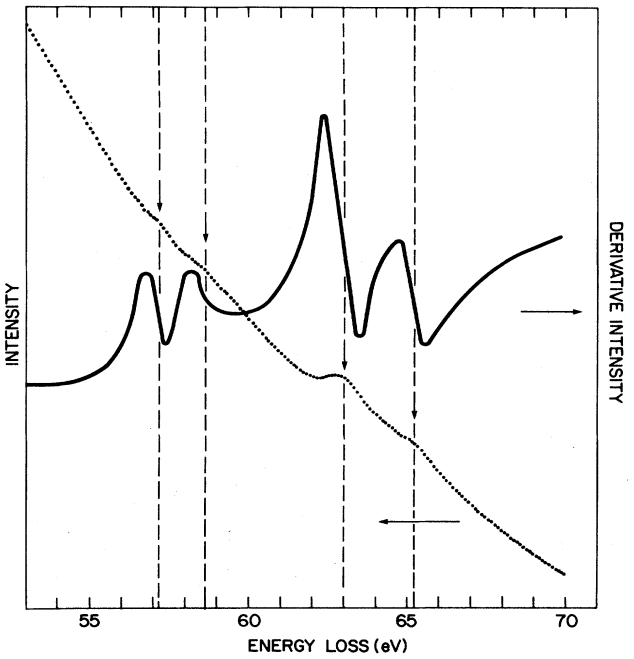

FIG. 4. Li 1*s* core-excitation and derivative spectra for LiC_6.

Information complementary to that contained in the C 1*s* data may be obtained from analysis of the Li 1*s* core edge, which probes the *p*-symmetry final states in the vicinity of the Li atoms. Figure 4 shows our measured edge shape and also the derivative curve. Four small peaks appear in the spectrum, arising from transitions from the sharp Li 1*s* level to peaks in the unoccupied density of states (DOS). Lacking a detailed theory to guide a line-shape fit, we estimate the transition energies as occurring at the inflection point of the derivative spectrum. For the third peak in the series, the procedure places the transition energy 0.2 eV above the zero slope in the direct spectrum, giving an estimate of ± 0.2 eV for the error involved in this procedure.

The very weak first peak at 57.1 ± 0.2 eV may be assigned to transitions to the lowest-lying unfilled states containing some Li character. We may estimate their position relative to the Fermi level by comparing the energy separation of the Li and C core-edge thresholds as measured by electron-energy-loss spectroscopy (EELS) and x-ray-photoemission spectroscopy (XPS). The XPS threshold corresponds to the energy of transitions to the vacuum (measured with respect to E_F), while the EELS threshold corresponds to transitions to the lowest unfilled states in the vicinity of the excited atom. Therefore, the difference (XPS—EELS) between the two respective C 1*s*—to—Li 1*s* threshold separations is equal to Δ, the energy above E_F of the Li unfilled-state threshold.[18] We write

$$\Delta = [\mathrm{C}(1s) - \mathrm{Li}(1s)]_{\mathrm{XPS}} - [\mathrm{C}(1s) - \mathrm{Li}(1s)]_{\mathrm{EELS}} ,$$

or, using published values of the XPS peaks,[19]

$$\Delta = (285.2 - 57.1)_{\mathrm{XPS}} - (285.1 - 57.1)_{\mathrm{EELS}} ,$$

or (in eV)

$$\Delta = 0.1 .$$

Since the four experimental numbers all have uncertainties of at least ± 0.1 eV, we find that $\Delta \simeq 0$ to within the experimental accuracies. Hence we assign the first weak peak in Fig. 4 at 57.1 as due to $\mathrm{Li}(1s) \rightarrow E_F$ dipole transitions. The small oscillator strength indicates only a small percentage of Li character for the states near E_F, as predicted by theory.[6] Such a Fermi threshold was actually undetectable for the K 2*p* core absorption in KC_8.[3] While one may draw the conclusion from this that the metal *s* hybridization is even smaller in KC_8 than in LiC_6, note that different final angular momenta are being probed, and that the possible Fermi threshold for K 2*p* is obscured by extended-loss structure of the C 1*s* absorption in the same energy range. Thus a direct comparison of the K 2*p* and Li 1*s* thresholds is not possible. The second feature in the Li 1*s* spectrum is also very weak and occurs at 58.7 ± 0.2 eV, or 1.6 eV above the first. We assign this feature to $\mathrm{Li}(1s) \rightarrow$ unoccupied conduction-band transitions. The small oscillator strength is expected since these would be dipole-forbidden transitions ($\Delta l = 0$) in a spherical potential. Such an assignment places the conduction-band minimum 1.6 eV above E_F, in agreement with the band-

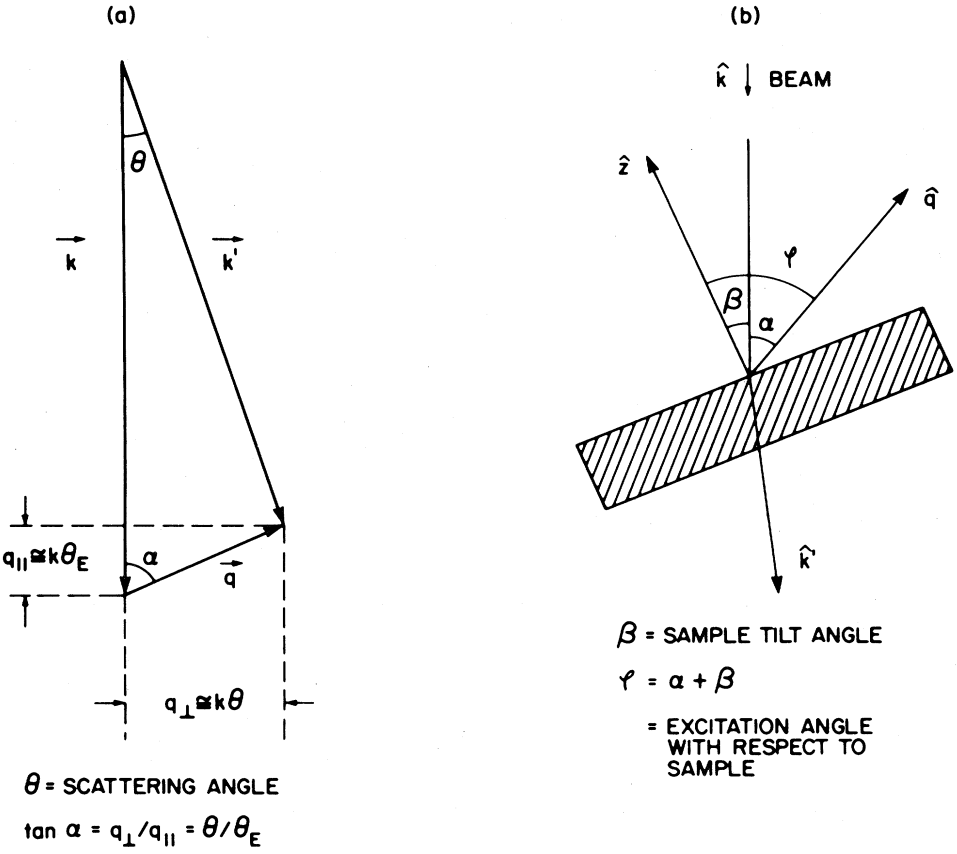

FIG. 5. Scattering kinematics and orientation angles in EELS. (Adapted from Ref. 23.)

structure calculation of Holzwarth *et al.*,[6,7] which shows a primarily Li-derived three-dimensional band of unfilled states extending down to 1.6 eV above E_F. Structure at similar energy above E_F is also predicted by the theory of Posternak *et al.*[5] A feature analogous to this excitation has been recently observed using inverse photoemission spectroscopy,[10] although this latter experiment infers the conduction-band minimum position to be almost 1 eV lower.

The next two features in the Li 1*s* spectrum at 63.0 and 65.2 eV (5.9 and 8.1 eV referenced to E_F) are considerably stronger. In identifying these absorption bands it is useful to compare the LiC_6 spectrum with that of pure Li.[20] The Li metal spectrum shows a sharp threshold at 55.0 eV, corresponding to transitions to E_F, followed by an unidentified peak at ~ 58 eV, and a large, broad hump centered at ~ 64 eV, corresponding to the dipole $1s \rightarrow 2p$ transitions. From this last energy we are led to assign the two strong features in the LiC_6 spectrum, with dipole-allowed transitions from the Li 1*s* core to the Li(2*p*)-derived states. The splitting reflects a crystal-field splitting of these atomiclike states by the C planes into lower-lying $2p_{xy}$ and higher-lying $2p_z$ levels. To confirm this, we study the orientational dependence of the 63.0- and 65.2-eV excitations.[21] The appropriate dipole form of the core-level EELS cross section is[22]

$$\frac{d^2\sigma_{if}}{d\Omega\, dE} = \frac{4}{a_0^2 q^4} |\langle f | \vec{q}\cdot\vec{r} | i \rangle|^2 ,$$

where $\hbar\vec{q}$ is the momentum transfer, a_0 is the Bohr radius, and the initial and final states are normalized per unit energy. For the Li 1*s* excitation, the initial state has spherical symmetry. Therefore, the excitation cross section will be maximized when $\vec{q}$ is parallel to the direction of maximum probability density of the final state, in this case, the Li $2p_{xy}$ or $2p_z$ states. As shown in Fig. 5(a),[23] $\vec{q}$ may be decomposed into components parallel and perpendicular to the incident-beam direction where

$$q_{\perp} \simeq k\theta$$

and

$$q_{\parallel} \simeq k[E/(2E_0)] \equiv k\theta_E .$$

Here $\hbar k$ and E_0 are the incident-electron momentum and energy, respectively, θ is the scattering angle, and E is the measured energy loss. $q_{\parallel}$ is determined by energy conservation, while $q_{\perp}$ is experimentally selected. The orientation being probed is determined by α, the angle between $\vec{k}$ and $\vec{q}$, given by

$$\alpha = \tan^{-1}(\theta/\theta_E) .$$

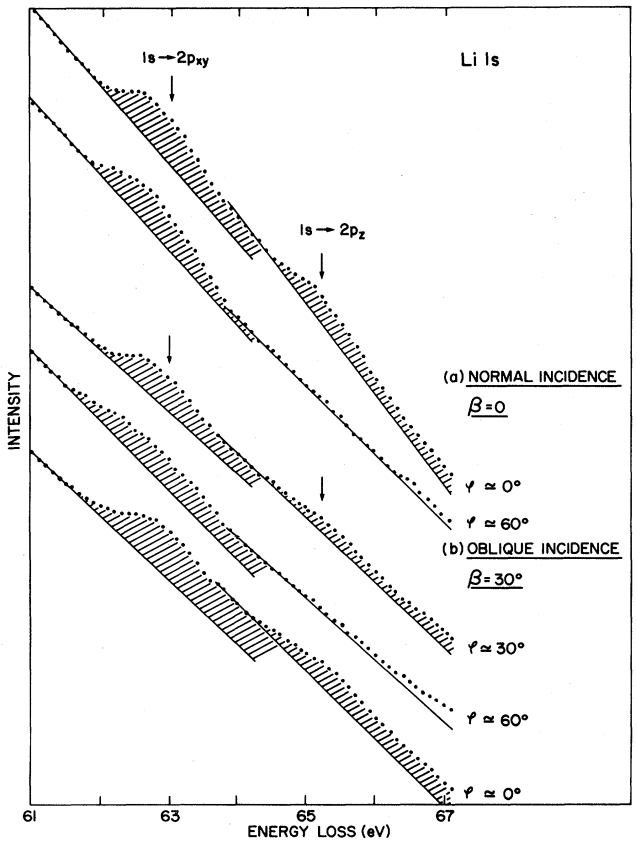

FIG. 6. Li 1s spectra for LiC_6 as a function of excitation orientation for (a) normal-incidence and (b) oblique-incidence beam.

In addition, the specimen may be tilted by an angle β with respect to the incident-beam direction, as shown in Fig. 5(b).[23] The total angle between $\vec{q}$ and the sample z axis (perpendicular to the C planes) is then given by

$$\varphi=\alpha+\beta\ .$$

At normal incidence ($\beta=0$) and $q_\perp=0$, we have $\theta=0$, and hence $\varphi=0$. Therefore, we should be probing excitations to states with maximum probability density along the z (or graphite C) axis. However, in the corresponding $\varphi=0$ spectrum of Fig. 6(a) both peaks labeled as transitions to the $2p_{xy}$ and $2p_z$ states appear. This is because the $q_\perp$ resolution of our spectrometer is of the same order of magnitude as $q_{||}$ for the Li 1s edge. However, by employing a $q_\perp=0.1$ Å^{-1}, we *increase* φ to $\sim 60°$ away from the sample z axis, and hence *decrease* the relative strength of the $2p_z$ to the $2p_{xy}$ final-state excitations, as confirmed in the lower curve of Fig. 6(a). An equivalent and symmetric way of performing this experiment consists of tilting the samples by $\beta=30°$ and then to measure the spectrum at $q_\perp=0$ and also at $\pm q_\perp$ values corresponding to angles $\alpha=\pm 30°$. This yields probe orientational angles φ of 30° ($q_\perp=0$), 60° ($q_\perp\simeq+0.3$ Å^{-1}), and 0° ($q_\perp\simeq-0.3$ Å^{-1}). The results are shown in Fig. 6(b), where once again the strength of the Li $1s\rightarrow 2p_z$ excitation *decreases* relative to the Li $1s\rightarrow 2p_{xy}$ excitation as φ *increases*. Thus we have provided evidence that the 63.0- and 65.2-eV features in the Li 1s spectrum correspond to transitions to the crystal-field-split components of the Li 2p states. These features are essentially atomic in origin, and are not manifestations of hybridization between Li and C, which may be responsible for the observed shape of the C 1s edge threshold. However, these higher-energy excitations are difficult to identify in a band-structure calculation[6,7] since many other bands of different character lie in the same energy range. Our experiment indicates that an appropriate theoretical projection of the total DOS into Li 2p states would reveal well-defined energies for $2p_{xy}$ and $2p_z$ character.

Electron-energy-loss measurements for LiC_6 enable us to probe various properties of the empty-state manifold. We conclude that the alkali-graphite compounds have empty states of identifiable alkali and C character. The lack of fine structure in the (15—40)-eV range in LiC_6 supports the picture of an unoccupied C 3p band, which, because of Brillouin-zone folding effects, is strongly optically assessable from C $2p_\pi$ bands for MC_8 compounds but not for LiC_6. Such a lack of fine structure has also recently been seen in BaC_6,[24] a compound with the same superlattice structure as LiC_6. Li 1s absorption demonstrates the presence of distinct Li 2p states above E_F. The polarization dependence of this absorption proves that this 2p state is split into a lower-lying $2p_{xy}$ state 5.9 eV above E_F and a higher-lying $2p_z$ state 8.1 eV above E_F. Thus the Li 2p manifold is apparently split by the local anisotropic crystal field but does not have significant bandwidth. Li 1s absorption also indicates the presence of a conduction band 1.6 eV above E_F. Inverse photoemission studies have also seen this interlayer band, but place it about 1 eV closer to E_F. The origin of this discrepancy is not clear, although it may be that the identification of our absorption peak with the band minimum is not quantitatively correct, or that the extrapolation of the inverse photoemission data to $k=0$ is inaccurate. In any case, our observation is incapable of addressing the present theoretical controversy of whether this interlayer band originates from Li or C states. Finally, it is possible that a careful analysis of the C 1s absorption edge could provide additional information about final states close to E_F. However, given the similarity of the LiC_6 with the MC_8 spectra, it seems more likely that this line shape is a manifestation of C conduction-electron relaxation effects than of any specific details of the one-electron unoccupied states.

The work at the University of Pennsylvania was supported by the National Science Foundation Materials Research Laboratory Program under Grant No. DMR-79-23647.

*Present address: IBM Thomas J. Watson Research Center, P.O. Box 218, Yorktown Heights, NY 10598.

[1]E. Cartier, F. Heinrich, P. Pfluger, and H. J. Güntherodt, Solid State Commun. 38, 985 (1981).

[2]U. M. Gubler, P. Oelhafen, and H. J. Güntherodt, Solid State Commun. 44, 1621 (1982).

[3]J. J. Ritsko and C. F. Brucker, Solid State Commun. 44, 889 (1982), and references therein.

[4]W. Eberhardt, J. T. McGovern, E. W. Plummer, and J. E. Fischer, Phys. Rev. Lett. 44, 200 (1980).

[5]M. Posternak, A. Baldereschi, A. J. Freeman, E. Wimmer, and M. Weinert, Phys. Rev. Lett. 50, 761 (1983).

[6]N. A. W. Holzwarth, S. Rabii, and L. A. Girifalco, Phys. Rev. B 18, 5190 (1978).

[7]N. A. W. Holzwarth, S. Louie, and S. Rabii, Phys. Rev. B 28, 1013 (1983).

[8]J. J. Ritsko, E. J. Mele, and I. P. Gates, Phys. Rev. B 24, 6114 (1981).

[9]L. A. Grunes and J. J. Ritsko, Phys. Rev. B 28, 3439 (1983).

[10]Th. Fauster, F. J. Himpsel, J. E. Fischer, and E. W. Plummer, Phys. Rev. Lett. 51, 430 (1983).

[11]M. E. Preil and J. E. Fischer (unpublished); J. M. Bloch (unpublished).

[12]S. Basu, C. Zeller, P. J. Flanders, C. D. Fuerst, W. D. Johnson, and J. E. Fischer, Mater. Sci. Eng. 38, 275 (1979); P. Pfluger, E. Schuppler, R. Lapka, and H. J. Güntherodt, in *Extended Abstracts of the 15th Biennial Conference on Carbon, June, 1981,* edited by W. C. Forsman (American Carbon Society, University Park, Pennsylvania, 1981), p. 70; P. Pfluger and H. J. Güntherodt, in *Festkörperprobleme (Advances in Solid State Physics),* edited by J. Treusch (Vieweg, Braunschweig, 1981), Vol. 21, p. 271.

[13]J. J. Ritsko, Phys. Rev. B 25, 6452 (1982).

[14]Other samples prepared at 400 °C to minimize carbide formation did not display this weak feature, but did exhibit some stage-2 contribution to the valence spectrum.

[15]E. J. Mele and J. J. Ritsko, Phys. Rev. Lett. 43, 68 (1979).

[16]D. P. DiVincenzo and E. J. Mele (unpublished).

[17]L. Samuelson and I. P. Batra, J. Phys. C 13, 5105 (1980).

[18]For a more detailed justification of this procedure, see Ref. 3.

[19]G. K. Wertheim, P. M. Th. M. Van Attekum, and S. Basu, Solid State Commun. 33, 1127 (1980).

[20]P. C. Gibbons, J. J. Ritsko, and S. E. Schnatterley, Phys. Rev. B 10, 5017 (1974); J. J. Ritsko, Ph.D. thesis, Princeton University, 1974 (unpublished).

[21]Similar orientational studies of C 1*s* to σ and π states have already been performed. See Ref. 23 and R. D. Leapman and J. Silcox, Phys. Rev. Lett. 42, 1361 (1979).

[22]H. A. Bethe, Ann. Phys. (Leipzig) 5, 325 (1930).

[23]R. D. Leapman, P. L. Fejes, and J. Silcox, Phys. Rev. B 28, 2361 (1983).

[24]M. E. Preil, L. A. Grunes, and J. E. Fischer (unpublished).